We are IntechOpen, the world's leading publisher of Open Access books Built by scientists, for scientists

6,900
Open access books available

185,000
International authors and editors

200M
Downloads

Our authors are among the

154
Countries delivered to

TOP 1%
most cited scientists

12.2%
Contributors from top 500 universities



WEB OF SCIENCE™

Selection of our books indexed in the Book Citation Index in Web of Science™ Core Collection (BKCI)

Interested in publishing with us?
Contact book.department@intechopen.com

Numbers displayed above are based on latest data collected.
For more information visit www.intechopen.com



Chapter 6

Hydrodynamic and Heat Transfer Simulation of Fluidized Bed Using CFD

Osama Sayed Abd El Kawi Ali

Additional information is available at the end of the chapter

http://dx.doi.org/10.5772/52072

1. Introduction

The nuclear energy is suffering from the lack of public acceptance everywhere mainly due to the issues relating to reactor safety, economy and nuclear waste. The Fluidized Bed Nuclear Reactor (FBNR) concept has addressed these issues and tried to resolve such problems. The FBNR is small, modular and simple in design contributing to the economy of the reactor. It has inherent safety and passive cooling characteristics. Its spent fuel being small spherical elements may not be considered nuclear waste, and can be directly used as a source of radiation for applications in industry and agriculture resulting in reduced environmental impact [1].

With the increase of computational power, numerical simulation becomes an additional tool to predict the fluid dynamics and the heat transfer mechanism in multiphase flow. A numerical hydrodynamic and heat transfer model has been developed to simulate the gas fluidized bed. All of CFD, in one form or another, is based on the fundamental governing equations of fluid dynamics (continuity, momentum and energy equations). These equations speak physics. They are mathematical statements of three fundamental physical principals upon which all fluid dynamics is based: mass is conserved, Newton's second law and energy is conserved [2].

This chapter aims to study a mathematical modeling and numerical simulation of the hydrodynamics and heat transfer processes in a two-dimensional gas fluidized bed with a vertical uniform gas velocity at the inlet. The velocity, volume fraction, temperature distribution for gas phase and particle phase are calculated. Also, gas pressure and a prediction of the average heat transfer coefficient are also studied.

Such a simulation technique allows performance evaluation for different bed input parameters, and can evolve into a tool for optimized design of fluidized beds for different industrial use.

INTECH
open science | open minds

© 2013 Abd El Kawi Ali; licensee InTech. This is an open access article distributed under the terms of the Creative Commons Attribution License (http://creativecommons.org/licenses/by/3.0), which permits unrestricted use, distribution, and reproduction in any medium, provided the original work is properly cited.

The numerical setup consists of a two dimensional fluidized bed filled with particles.The cold gas enters to the bed to cool the hot particles. Based on conservation equations for both phases it is possible to predict particles and gas volume fractions, velocity distributions (for gas and particles), temperature distribution, heat transfer coefficient as well as gas pressure field.

2. General assumptions for the mathematical model

Fluidized beds are categorized as multiphase flow problems. There are currently two approaches to model multiphase flow problems as discussed in chapter two. The best overall balance between computational time and accuracy seems to be achieved by implementing an Eulerian-Eulerian approach. The following assumptions are introduced into the present analysis:

1. The bed is two-dimensional.
2. Eulerian-Eulerian approach is applied.
3. The gas has constant physical properties.
4. Uniform fluidization.
5. Constant input fluid flux.
6. There is no mass transfer or chemical reaction between the two phases.
7. All particles are spherical in shape with the same diameter,d_p.
8. The expanded bed region is considered in the analysis in addition to the out flowing gas, i.e. suspension and free board regions.
9. Viscous heat dissipation in the energy equation is negligible in comparison with conduction and convection.

3. Governing equations

Due to the high particle concentration in fluidized beds the particles interactions cannot be neglected. In fact the solid phase has similar properties as continuous fluid. Therefore, the Eulerian approach is an efficient method for the numerical simulation of fluidized beds.

A hydrodynamic and thermal model for the fluidized bed is developed based on schematic diagram shown in Figure (1). The principles of conservation of mass, momentum, and energy are used in the hydrodynamic and thermal models of fluidization. The general mass conservation equations and the separate phase momentum equations and energy equations (for each phase) for fluid–solids, nonreactive transient and two-phase flow will be discussed in the following sections.

http://dx.doi.org/10.5772/52072

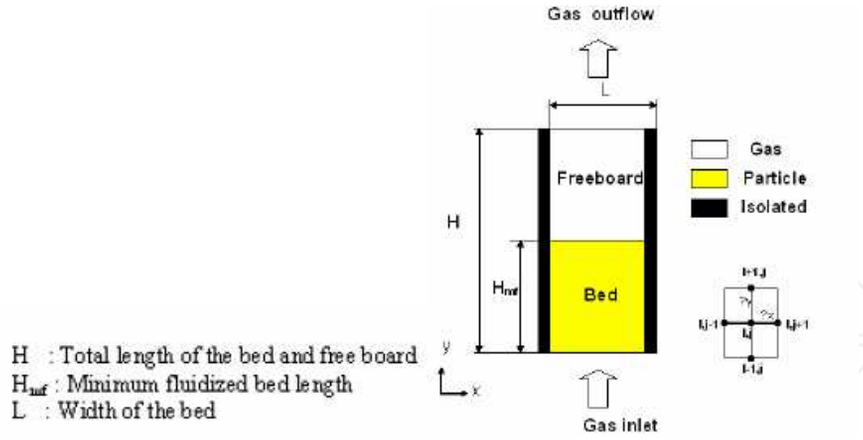


Figure 1. The schematic diagram of the present work model

3.1. Continuity equation

Particle phase:

$$\frac{\partial \varepsilon_s}{\partial t} + \frac{\partial}{\partial x}(\varepsilon_s u_s) + \frac{\partial}{\partial y}(\varepsilon_s v_s) = 0 \tag{1}$$

Gas phase :

$$\frac{\partial \varepsilon_g}{\partial t} + \frac{\partial}{\partial x}(\varepsilon_g u_g) + \frac{\partial}{\partial y}(\varepsilon_g v_g) = 0 \tag{2}$$

3.2. Volume fraction constraint

$$\varepsilon_g + \varepsilon_s = 1.0 \tag{3}$$

3.3. Momentum equation

Particle phase:

$$\rho_s \varepsilon_s \frac{\partial u_s}{\partial t} + \rho_s \varepsilon_s \frac{\partial}{\partial x}(u_s u_s) + \rho_s \varepsilon_s \frac{\partial}{\partial y}(v_s u_s) = F_{sx} \quad \text{“x -direction “} \tag{4}$$

$$\rho_s \varepsilon_s \frac{\partial v_s}{\partial t} + \rho_s \varepsilon_s \frac{\partial}{\partial x}(u_s v_s) + \rho_s \varepsilon_s \frac{\partial}{\partial y}(v_s v_s) = F_{sy} \quad \text{“y -direction “} \tag{5}$$

The total force acting on particle phase is the sum of the net primary force and the force resulting from particle phase elasticity. The x and y components of forces acting on particle phase are as following:

$$F_{sy} = C_d \frac{3\varepsilon_s \rho_g (v_g - v_s)\left|v_g - v_s\right|}{4d_p}(1-\varepsilon_s)^{-1.8} - \varepsilon_s \rho_s g$$
$$-\varepsilon_s \frac{\partial p}{\partial y} - \frac{\partial \varepsilon_s}{\partial y}(3.2 g d_p \varepsilon_s (\rho_s - \rho_g)) \tag{6}$$

$$F_{sx} = C_d \frac{3\varepsilon_s \rho_g (u_g - u_s)\left|u_g - u_s\right|}{4d_p}(1-\varepsilon_s)^{-1.8} - \varepsilon_s \frac{\partial p}{\partial x} \tag{7}$$

Gas phase :

$$\rho_g \varepsilon_g \frac{\partial u_g}{\partial t} + \rho_g \varepsilon_g \frac{\partial}{\partial x}(u_g u_g) + \rho_g \varepsilon_g \frac{\partial}{\partial y}(v_g u_g) = F_{gx} \text{ “x -direction “} \tag{8}$$

$$\rho_g \varepsilon_g \frac{\partial v_g}{\partial t} + \rho_g \varepsilon_g \frac{\partial}{\partial x}(u_g v_g) + \rho_g \varepsilon_g \frac{\partial}{\partial y}(v_g v_g) = F_{gy} \text{ “y -direction “} \tag{9}$$

The fluid phase forces are readily obtained from the particle phase relations for fluid – particle interaction (drag and pressure gradient force), which act in the opposite direction on the fluid, together with gravity. The x and y components of forces acting on gas phase are as following:

$$F_{gy} = -C_d \frac{3\varepsilon_s \rho_g (v_g - v_s)\left|v_g - v_s\right|}{4d_p}(1-\varepsilon_s)^{-1.8} - \varepsilon_g \rho_s g - \varepsilon_g \frac{\partial p}{\partial y} \tag{10}$$

$$F_{gx} = -F_{sx} = -C_d \frac{3\varepsilon_s \rho_g (u_g - u_s)\left|u_g - u_s\right|}{4d_p}(1-\varepsilon_s)^{-1.8} + \varepsilon_s \frac{\partial p}{\partial x} \tag{11}$$

3.3.1. Relation between fluid and particle velocities

We assume that both particles and fluid are regarded as being incompressible. This was justified on the basis that only a gas phase is going to exhibit any significant compressibility, and the orders of magnitude differences in particle and fluid density for gas fluidization render quite insignificant the small change in gas density resulting from compression. This assump-

http://dx.doi.org/10.5772/52072

tion led to the relation linking fluid and particle phase velocities at all location. By applying the overall mass balance, which is obtained by summing equations (1) and (2):

$$\frac{\partial}{\partial x}(\varepsilon_s u_s + \varepsilon_g u_g) + \frac{\partial}{\partial y}(\varepsilon_s v_s + \varepsilon_g v_g) = 0 \tag{12}$$

Equation (12) shows that the total flux (fluid plus particles) in x- direction and y-direction remains constant, equal to that of fluid entering the bed U_{gin},V_{gin}. This result is a simple consequence of the particles and fluid being considered incompressible :

$$V_{gin} = \varepsilon_g v_g + \varepsilon_s v_s \tag{13}$$

$$U_{gin} = \varepsilon_g u_g + \varepsilon_s u_s \tag{14}$$

Equations (13) and (14) enable the fluid velocity variables to be expressed in terms of the particle velocity at all points in the bed.

3.3.2. Combined momentum equation

In this section the combined momentum equation is produced by combining the fluid and particle momentum equations (4), (5), (8) and (9) by elimination of the fluid pressure gradient, which appears in them. This yields the combined momentum equation:

x- direction:

[divide equation (4-4) by ε_s] + [divide equation (4-8) by ε_g] which give us :

$$\rho_s\left[\frac{\partial u_s}{\partial t} + \frac{\partial}{\partial x}(u_s u_s) + \frac{\partial}{\partial y}(v_s u_s)\right] + \rho_g\left[\frac{\partial u_s}{\partial t} + \frac{\partial}{\partial x}(u_g u_g) + \frac{\partial}{\partial y}(v_g u_g)\right] = 0 \tag{15}$$

y- direction:

[divide equation (4-3) by ε_s] – [divide equation (4-7) by ε_g] which give us :

$$\rho_s\left[\frac{\partial v_s}{\partial t} + \frac{\partial}{\partial x}(u_s v_s) + \frac{\partial}{\partial y}(v_s v_s)\right]$$

$$-\rho_g\left[\frac{\partial v_g}{\partial t} + \frac{\partial}{\partial x}(u_g v_g) + \frac{\partial}{\partial y}(v_g v_g)\right] = \frac{F_{sy}}{\varepsilon_s} - \frac{F_{gy}}{\varepsilon_g} \tag{16}$$

Equations (15) and (16) with the continuity equation for the two phase (1) and (2),now define the two phase system without account of fluid pressure variation.

3.3.3. Drag coefficient

An important constitutive relation in any multiphase flow model is the formula for the fluid-particle drag coefficient, which is may be expressed by the empirical Dallavalle relation as reported in [3] :

$$C_d = \left(0.63 + \frac{4.8}{\mathrm{Re}^{0.5}} \right)^2 \tag{17}$$

The particle Reynolds number, Re, based on particle diameter is given by :

$$\mathrm{Re} = \frac{\varepsilon_g \rho_g d_p \left| \overrightarrow{U_r} \right|}{\mu_g} \tag{18}$$

3.3.4. Gas pressure drop

Figure (2) shows the relation between the total pressure drop across the bed "ΔP_B" and the input gas velocity [3].where:

$$\Delta P_B = \left(\rho_g \varepsilon_{g,mf} + \rho_s \left(1 - \varepsilon_{g,mf} \right) \right) g H_{mf} \tag{19}$$

The gas pressure at the entrance of the fluidized bed can be calculated from the following equation:

$$P_{g,in} = P_{atm} + \rho_g g \left(H - H_{mf} \right) + \left(\rho_g \varepsilon_{g,mf} + \rho_s \left(1 - \varepsilon_{g,mf} \right) \right) g H_{mf} \tag{20}$$

and the pressure drop at any position and head "h" can be calculated from:

$$\Delta P_g = \rho_{sus} g h \tag{21}$$

Where $\rho_{sus}$is the suspension density which calculated from:

$$\rho_{sus} = \rho_s \varepsilon_s + \rho_g \varepsilon_g \tag{22}$$

http://dx.doi.org/10.5772/52072

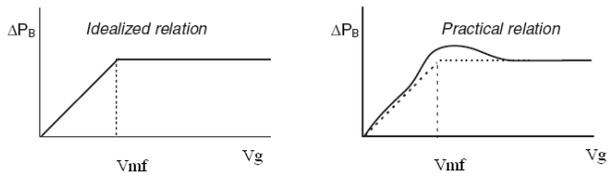


Figure 2. Total pressure drop in fluidized bed

3.4. Energy equation

Particle phase:

$$\rho_s C_{ps} \frac{\partial \varepsilon_s T_s}{\partial t} + \rho_s C_{ps} \frac{\partial}{\partial x}(\varepsilon_s u_s T_s) + \rho_s C_{ps} \frac{\partial}{\partial y}(\varepsilon_s v_s T_s) = \frac{\partial}{\partial x}(\varepsilon_s k_s \frac{\partial T_s}{\partial x}) + \frac{\partial}{\partial y}(\varepsilon_s k_s \frac{\partial T_s}{\partial y}) + h_v(T_g - T_s) + \varepsilon_s \dot{q} \tag{23}$$

GAS phase:

$$\rho_g C_{pg} \frac{\partial \varepsilon_g T_g}{\partial t} + \rho_g C_{pg} \frac{\partial}{\partial x}(\varepsilon_g u_g T_g) + \rho_g C_{pg} \frac{\partial}{\partial y}(\varepsilon_g v_g T_g) = \frac{\partial}{\partial x}(\varepsilon_g k_g \frac{\partial T_g}{\partial x}) + \frac{\partial}{\partial y}(\varepsilon_g k_g \frac{\partial T_g}{\partial y}) + h_v(T_s - T_g) \tag{24}$$

3.4.1. Thermal conductivity values (k_g and k_s)

The thermal conductivities of the fluid phase and the solid phase (k_g and k_s) in the two fluid model formulation should be interpreted as effective transport coefficients which means that the corresponding microscopic (or absolute) coefficients $k_{g,o}$ and $k_{s,o}$ cannot be used. It can be represented in general as:

$$k_g = k_g(k_{g,o}, k_{s,o}, \varepsilon_g, \text{ particle geometry}) \tag{25}$$

$$k_s = k_s(k_{g,o}, k_{s,o}, \varepsilon_g, \text{ particle geometry}) \tag{26}$$

However, such a general formulation is not yet available for fluidized beds and approximate constitutive equations have to be used. These approximate equations have been obtained on modeling of the effective thermal conductivity k_b in packed beds. According to their model,

the radial bed conductivity k_b consists of a contribution $k_{b,g}$ due to the fluid phase only and a contribution due to a combination of the fluid phase and the solid phase[4].

$$k_b = k_{b,g} + k_{b,s} \tag{27}$$

where :

$$k_{bg} = \left(1 - \sqrt{1-\varepsilon_g}\right) k_{go} \tag{28}$$

$$k_{bs} = \sqrt{1-\varepsilon_g}\left(\omega A + (1-\omega)\Gamma\right) k_{go} \tag{29}$$

$$\Gamma = \frac{2}{\left(1-\frac{B}{A}\right)}\left[\frac{A-1}{\left(1-\frac{B}{A}\right)^2}\frac{B}{A} Ln\left(\frac{A}{B}\right) - \frac{B-1}{\left(1-\frac{B}{A}\right)} - \frac{1}{2}(B+1)\right] \tag{30}$$

$$B = 1.25\left(\frac{1-\varepsilon_g}{\varepsilon_g}\right)^{\frac{10}{9}} \tag{31}$$

$$A = \frac{k_{s,o}}{k_{g,o}} \tag{32}$$

$$\omega = 7.26X10^{-3} \tag{33}$$

Thus the thermal conductivities of the fluid phase and the solid phase then are given by :

$$k_g = \frac{k_{b,g}}{\varepsilon_g} \tag{34}$$

$$k_s = \frac{k_{b,s}}{\varepsilon_s} \tag{35}$$

http://dx.doi.org/10.5772/52072

3.4.2. Interphase volumetric heat transfer coefficient h_v

The heat transfer coefficient is modelled using a correlation by Gunn as reported [5]. This correlation is applicable for gas voidage in the range of 0.35 to 1 and for Reynolds numbers up to Re = 10^5, and gives the Nusselt number:

$$Nu = \frac{h_{gp} d_p}{k_{g,o}} \tag{36}$$

$$Nu = \left(7 - 10\varepsilon_g + 5\varepsilon_g^2\right)\left(1 + 0.7\mathrm{Re}_p^{0.2}\mathrm{Pr}^{\frac{1}{3}}\right)$$

$$+ \left(1.33 - 2.40\varepsilon_g + 1.20\varepsilon_g^2\right)\mathrm{Re}_p^{0.7}\,\mathrm{Pr}^{\frac{1}{3}} \tag{37}$$

where Reynolds number is defined by equation (18).The Prandlt number is defined by;

$$\mathrm{Pr} = \frac{C_{p,g}\mu_g}{k_{g,o}} \tag{38}$$

,and the overall heat transfer coefficient is evaluated from;

$$h_v = \frac{6\left(1 - \varepsilon_g\right)h_{gp}}{d_p} \tag{39}$$

4. Boundary and initial conditions

The system of conservation equations (1),(2), (3), (4), (5), (8), (9), (23), and (24), nine equations which are discussed in previous sections must be solved for the nine dependent variables: the gas-phase volume fraction ε_g, the particle-phase volume fraction ε_s, the gas pressure P_g, the gas velocity components u_g and v_g and the solids velocity components u_s and v_s in x-direction and y-direction, respectively,the gas temperature T_g and particle temperature T_s.We need appropriate boundary and initial conditions for the dependent variables listed above to solve the system of equations.

4.1. Boundary conditions

In this section the boundary conditions for the above governing equations, which relate to two dimensional fluidized bed with width "L" and height "H" to allow bed expansion typically i.e. the height of the bed is enough to prevent the particles being ejected from the bed. Boundary conditions are imposed as follow:

$$x=0 \quad : v_g = v_s = u_g = u_s = 0, \qquad \frac{\partial \varepsilon_g}{\partial x} = \frac{\partial T_g}{\partial x} = \frac{\partial T_s}{\partial x} = 0$$

$$x=\frac{L}{2} \quad : \frac{\partial \varepsilon_g}{\partial x} = \frac{\partial T_g}{\partial x} = \frac{\partial T_s}{\partial x} = \frac{\partial v_g}{\partial x} = \frac{\partial u_g}{\partial x} = \frac{\partial v_s}{\partial x} = \frac{\partial u_s}{\partial x} = 0 \quad (symmetric)$$

$$y=0 \quad : v_g = V_{g,in}, \quad u_g = u_s = v_s = 0, \quad \varepsilon_g = 1, \quad P_g = P_{g,in}, \quad T_g = T_{g,in}, \quad \frac{\partial T_s}{\partial y} = 0$$

$$y=H : \frac{\partial v_g}{\partial y} = \frac{\partial u_g}{\partial y} = \frac{\partial T_g}{\partial y} = 0, \quad \varepsilon_g = 1, \quad v_s = u_s = 0, \quad P_g = P_{atm}$$

4.2. Initial conditions

For setting the initial conditions, the model is divided into two regions: the bed and the freeboard. For each of the regions specified above, an initial condition is specified.

Bed region

$$\varepsilon_g = \varepsilon_{g,mf}, \quad v_g = \frac{V_{g,mf}}{\varepsilon_{g,mf}}, \quad u_g = v_s = u_s = 0, \quad T_g = T_{g,in}, \quad T_s = T_{s,in}$$

Freeboard region

$$\varepsilon_g = 1, \quad v_g = V_{g,mf}, \quad u_g = v_s = u_s = 0, \quad T_g = T_{g,in}$$

5. Finite difference approximation scheme

The conservation equations are transformed into difference equations by using a finite difference scheme.

5.1. Discretization of continuity equations

5.1.1. Particle phase continuity equation

The particle phase continuity equation,Eq.(1), is discretized at the node i; j in an explicit form as:

$$\begin{aligned}\left(\varepsilon_s\right)_{i,j}^{n+1} = \left(\varepsilon_s\right)_{i,j}^{n} &- \frac{\Delta t}{\Delta x}\left(u_s\right)_{i,j}^{n} \begin{cases} \left(\varepsilon_s\right)_{i,j}^{n} - \left(\varepsilon_s\right)_{i-1,j}^{n} & ,if \left(u_s\right)_{i,j}^{n} \geq 0.0 \\ \left(\varepsilon_s\right)_{i+1,j}^{n} - \left(\varepsilon_s\right)_{i,j}^{n} & ,if \left(u_s\right)_{i,j}^{n} < 0.0 \end{cases} \\ &- \frac{\Delta t}{\Delta y}\left(v_s\right)_{i,j}^{n} \begin{cases} \left(\varepsilon_s\right)_{i,j}^{n} - \left(\varepsilon_s\right)_{i,j-1}^{n} & ,if \left(v_s\right)_{i,j}^{n} \geq 0.0 \\ \left(\varepsilon_s\right)_{i,j+1}^{n} - \left(\varepsilon_s\right)_{i,j}^{n} & ,if \left(v_s\right)_{i,j}^{n} < 0.0 \end{cases}\end{aligned} \tag{40}$$

The gas phase volume fraction is then calculated explicitly as:

http://dx.doi.org/10.5772/52072

$$\left(\varepsilon_g\right)_{i,j}^{n+1} = 1 - \left(\varepsilon_s\right)_{i,j}^{n+1} \tag{41}$$

5.1.2. Gas phase continuity equation

The gas continuity equation residual, d_g, is discretized at i; j in a fully implicit way:

$$\begin{aligned} d_g = \left(\varepsilon_g\right)_{i,j}^{n+1} - \left(\varepsilon_g\right)_{i,j}^{n} + \frac{\Delta t}{\Delta x}\left(u_g\right)_{i,j}^{n+1} \begin{cases} \left(\varepsilon_g\right)_{i,j}^{n+1} - \left(\varepsilon_g\right)_{i-1,j}^{n+1} & ,if\left(u_g\right)_{i,j}^{n+1} \geq 0.0 \\ \left(\varepsilon_g\right)_{i+1,j}^{n+1} - \left(\varepsilon_g\right)_{i,j}^{n+1} & ,if\left(u_g\right)_{i,j}^{n+1} < 0.0 \end{cases} \\ + \frac{\Delta t}{\Delta y}\left(v_g\right)_{i,j}^{n+1} \begin{cases} \left(\varepsilon_g\right)_{i,j}^{n+1} - \left(\varepsilon_g\right)_{i,j-1}^{n+1} & ,if\left(v_g\right)_{i,j}^{n+1} \geq 0.0 \\ \left(\varepsilon_g\right)_{i,j+1}^{n+1} - \left(\varepsilon_g\right)_{i,j}^{n+1} & ,if\left(v_g\right)_{i,j}^{n+1} < 0.0 \end{cases} \end{aligned} \tag{42}$$

5.2. Discretization of combined momentum equations

The combined momentum equations may after a time discretization be expressed in the following forms for x and y directions:

x –direction:

$$\begin{aligned} & \rho_s \left[\frac{\left(u_s\right)_{i,j}^{n+1} - \left(u_s\right)_{i,j}^{n}}{\Delta t} + \frac{\left(u_s\right)_{i,j}^{n}}{\Delta x} \begin{cases} \left(u_s\right)_{i,j}^{n} - \left(u_s\right)_{i-1,j}^{n} & ,if\left(u_s\right)_{i,j}^{n} \geq 0.0 \\ \left(u_s\right)_{i+1,j}^{n} - \left(u_s\right)_{i,j}^{n} & ,if\left(u_s\right)_{i,j}^{n} < 0.0 \end{cases} \right] \\ & + \rho_s \left[\frac{\left(v_s\right)_{i,j}^{n}}{\Delta y} \begin{cases} \left(u_s\right)_{i,j}^{n} - \left(u_s\right)_{i,j-1}^{n} & ,if\left(v_s\right)_{i,j}^{n} \geq 0.0 \\ \left(u_s\right)_{i,j+1}^{n} - \left(u_s\right)_{i,j}^{n} & ,if\left(v_s\right)_{i,j}^{n} < 0.0 \end{cases} \right] \\ & + \rho_g \left[\frac{\left(u_g\right)_{i,j}^{n+1} - \left(u_g\right)_{i,j}^{n}}{\Delta t} + \frac{\left(u_g\right)_{i,j}^{n}}{\Delta x} \begin{cases} \left(u_g\right)_{i,j}^{n} - \left(u_g\right)_{i-1,j}^{n} & ,if\left(u_g\right)_{i,j}^{n} \geq 0.0 \\ \left(u_g\right)_{i+1,j}^{n} - \left(u_g\right)_{i,j}^{n} & ,if\left(u_g\right)_{i,j}^{n} < 0.0 \end{cases} \right] \\ & + \rho_g \left[\frac{\left(v_g\right)_{i,j}^{n}}{\Delta y} \begin{cases} \left(u_g\right)_{i,j}^{n} - \left(u_g\right)_{i,j-1}^{n} & ,if\left(v_g\right)_{i,j}^{n} \geq 0.0 \\ \left(u_g\right)_{i,j+1}^{n} - \left(u_g\right)_{i,j}^{n} & ,if\left(v_g\right)_{i,j}^{n} < 0.0 \end{cases} \right] = 0 \end{aligned} \tag{43}$$

y –direction:

$$\rho_s\left[\frac{\left(v_s\right)_{i,j}^{n+1}-\left(v_s\right)_{i,j}^{n}}{\Delta t}+\frac{\left(u_s\right)_{i,j}^{n}}{\Delta x}\begin{cases}\left(v_s\right)_{i,j}^{n}-\left(v_s\right)_{i-1,j}^{n} & ,if\left(u_s\right)_{i,j}^{n}\geq 0.0\\ \left(v_s\right)_{i+1,j}^{n}-\left(v_s\right)_{i,j}^{n} & ,if\left(u_s\right)_{i,j}^{n}<0.0\end{cases}\right]$$
$$+\rho_s\left[\frac{\left(v_s\right)_{i,j}^{n}}{\Delta y}\begin{cases}\left(v_s\right)_{i,j}^{n}-\left(v_s\right)_{i,j-1}^{n} & ,if\left(v_s\right)_{i,j}^{n}\geq 0.0\\ \left(v_s\right)_{i,j+1}^{n}-\left(v_s\right)_{i,j}^{n} & ,if\left(v_s\right)_{i,j}^{n}<0.0\end{cases}\right]$$
$$-\rho_g\left[\frac{\left(v_g\right)_{i,j}^{n+1}-\left(v_g\right)_{i,j}^{n}}{\Delta t}+\frac{\left(u_g\right)_{i,j}^{n}}{\Delta x}\begin{cases}\left(v_g\right)_{i,j}^{n}-\left(v_g\right)_{i-1,j}^{n} & ,if\left(u_g\right)_{i,j}^{n}\geq 0.0\\ \left(v_g\right)_{i+1,j}^{n}-\left(v_g\right)_{i,j}^{n} & ,if\left(u_g\right)_{i,j}^{n}<0.0\end{cases}\right] \tag{44}$$
$$-\rho_g\left[\frac{\left(v_g\right)_{i,j}^{n}}{\Delta y}\begin{cases}\left(v_g\right)_{i,j}^{n}-\left(v_g\right)_{i,j-1}^{n} & ,if\left(v_g\right)_{i,j}^{n}\geq 0.0\\ \left(v_g\right)_{i,j+1}^{n}-\left(v_g\right)_{i,j}^{n} & ,if\left(v_g\right)_{i,j}^{n}<0.0\end{cases}\right]=F_y$$

where:

$$F_y=\left(C_d\right)_{i,j}^{n}\frac{3\rho_g\left(\left(v_g\right)_{i,j}^{n+1}-\left(v_s\right)_{i,j}^{n+1}\right)\left|\left(v_g\right)_{i,j}^{n}-\left(v_s\right)_{i,j}^{n}\right|}{4d_p}\left(1-\left(\varepsilon_s\right)_{i,j}^{n}\right)^{-1.8}$$
$$-\frac{\left(\varepsilon_s\right)_{i,j}^{n}-\left(\varepsilon_s\right)_{i,j-1}^{n}}{\Delta y}\left(3.2gd_p\left(\rho_s-\rho_g\right)\right) \tag{45}$$
$$+\left(C_d\right)_{i,j}^{n}\frac{3\rho_g\left(\varepsilon_s\right)_{i,j}^{n}\left(\left(v_g\right)_{i,j}^{n+1}-\left(v_s\right)_{i,j}^{n+1}\right)\left|\left(v_g\right)_{i,j}^{n}-\left(v_s\right)_{i,j}^{n}\right|}{4d_p}\left(1-\left(\varepsilon_s\right)_{i,j}^{n}\right)^{-2.8}$$

5.3. Discretization of energy equations

Particle phase:

http://dx.doi.org/10.5772/52072

$$
\begin{aligned}
&\rho_s C_{p,s}\frac{\left(\varepsilon_s T_s\right)_{i,j}^{n+1}-\left(\varepsilon_s T_s\right)_{i,j}^{n}}{\Delta t}\\
&+\frac{\rho_s C_{p,s}\left(u_s\right)_{i,j}^{n}}{\Delta x}\begin{cases}\left(\varepsilon_s T_s\right)_{i,j}^{n}-\left(\varepsilon_s T_s\right)_{i-1,j}^{n} & ,if\left(u_s\right)_{i,j}^{n}\geq 0.0\\ \left(\varepsilon_s T_s\right)_{i+1,j}^{n}-\left(\varepsilon_s T_s\right)_{i,j}^{n} & ,if\left(u_s\right)_{i,j}^{n}<0.0\end{cases}\\
&+\frac{\rho_s C_{p,s}\left(v_s\right)_{i,j}^{n}}{\Delta y}\begin{cases}\left(\varepsilon_s T_s\right)_{i,j}^{n}-\left(\varepsilon_s T_s\right)_{i,j-1}^{n} & ,if\left(v_s\right)_{i,j}^{n}\geq 0.0\\ \left(\varepsilon_s T_s\right)_{i,j+1}^{n}-\left(\varepsilon_s T_s\right)_{i,j}^{n} & ,if\left(v_s\right)_{i,j}^{n}<0.0\end{cases}\\
&=\frac{\left(\varepsilon_s K_s T_s\right)_{i+1,j}^{n}-2\left(\varepsilon_s K_s T_s\right)_{i,j}^{n}+\left(\varepsilon_s K_s T_s\right)_{i-1,j}^{n}}{\Delta x^2}\\
&+\frac{\left(\varepsilon_s K_s T_s\right)_{i,j+1}^{n}-2\left(\varepsilon_s K_s T_s\right)_{i,j}^{n}+\left(\varepsilon_s K_s T_s\right)_{i,j-1}^{n}}{\Delta y^2}\\
&+\left(h_v\right)_{i,j}^{n+1}\left(\left(T_g\right)_{i,j}^{n+1}-\left(T_s\right)_{i,j}^{n+1}\right)+\left(\varepsilon_s \dot{q}\right)_{i,j}^{n}
\end{aligned}
\tag{46}
$$

Gas Phase:

$$
\begin{aligned}
&\rho_g C_{p,g}\frac{\left(\varepsilon_g T_g\right)_{i,j}^{n+1}-\left(\varepsilon_g T_g\right)_{i,j}^{n}}{\Delta t}\\
&+\frac{\rho_g C_{p,g}\left(u_g\right)_{i,j}^{n}}{\Delta x}\begin{cases}\left(\varepsilon_g T_g\right)_{i,j}^{n}-\left(\varepsilon_g T_g\right)_{i-1,j}^{n} & ,if\left(u_g\right)_{i,j}^{n}\geq 0.0\\ \left(\varepsilon_g T_g\right)_{i+1,j}^{n}-\left(\varepsilon_g T_g\right)_{i,j}^{n} & ,if\left(u_g\right)_{i,j}^{n}<0.0\end{cases}\\
&+\frac{\rho_s C_{p,g}\left(v_g\right)_{i,j}^{n}}{\Delta y}\begin{cases}\left(\varepsilon_g T_g\right)_{i,j}^{n}-\left(\varepsilon_g T_g\right)_{i,j-1}^{n} & ,if\left(v_g\right)_{i,j}^{n}\geq 0.0\\ \left(\varepsilon_g T_g\right)_{i,j+1}^{n}-\left(\varepsilon_g T_g\right)_{i,j}^{n} & ,if\left(v_g\right)_{i,j}^{n}<0.0\end{cases}\\
&=\frac{\left(\varepsilon_g K_g T_g\right)_{i+1,j}^{n}-2\left(\varepsilon_g K_g T_g\right)_{i,j}^{n}+\left(\varepsilon_g K_g T_g\right)_{i-1,j}^{n}}{\Delta x^2}\\
&+\frac{\left(\varepsilon_g K_g T_g\right)_{i,j+1}^{n}-2\left(\varepsilon_g K_g T_g\right)_{i,j}^{n}+\left(\varepsilon_g K_g T_g\right)_{i,j-1}^{n}}{\Delta y^2}\\
&+\left(h_v\right)_{i,j}^{n+1}\left(\left(T_s\right)_{i,j}^{n+1}-\left(T_g\right)_{i,j}^{n+1}\right)
\end{aligned}
\tag{47}
$$

6. Dimensionless numbers

In this section we define a group of four dimensionless numbers which mainly affect and control fluidization field.

6.1. Archimedes number" Ar"

Archimedes Number is used in characterization of the fluidized state and is defined as follow:

$$Ar = \frac{g d_p^3 \rho_g \left(\rho_s - \rho_g\right)}{\mu_g^2} \tag{48}$$

6.2. Density number "De"

Which define as the density ratio:

$$De = \frac{\rho_g}{\rho_s} \tag{49}$$

6.3. Flow number "fl"

Which is defined as:

$$fl = \frac{V_{g,in}}{u_t} \tag{50}$$

6.4. Dimensionless gas velocity "$\Omega^{1/3}$"

Which is defined as:

$$\Omega^{1/3} = \left[\frac{\rho_g^2}{\mu_g g\left(\rho_s - \rho_g\right)}\right]^{1/3} V_{g,in} \tag{51}$$

6.5. Dimensionless time "τ"

Which is defined as:

$$\tau = \frac{t u_t}{d_p} \tag{52}$$

http://dx.doi.org/10.5772/52072

7. Methodology of solution

The method of solution used in the present work is described in details in this section. The procedures of solution are as following:

1. Input the following parameters :

- Total time of calculation
- Total nodes number in x and y direction
- Total height of the bed and free board
- Width of fluidized bed
- Initial height of the bed
- Properties of gas phase ($\mu_g, \varrho_g, k_g, C_{p,g}$)
- Properties of solid particles phase ($\varrho_s, k_s, C_{p,s}$)
- Entering gas velocity
- Acceleration of gravity
- Particle diameter
- Entering gas temperature
- Initial particles temperature

2. Calculate the minimum fluidized velocity from the following equation [6] :

$$V_{g,mf} = 33.7\left[\left(1 + 3.59X10^{-5}\,Ar\right)^{0.5} - 1\right]\frac{\mu_g}{\left(d_p\rho_g\right)} \tag{53}$$

3. Calculate the gas void fraction at minimum fluidized velocity from the following equation [7]:

$$\in_{g,mf} = \frac{1}{2.1}[0.4 + (\frac{200\mu_g V_{g,mf}}{d_p^2(\rho_s - \rho_g)g})^{1/3}] \tag{54}$$

4. Calculate the gas void fraction at entering gas velocity which given by:

$$\in_{g,in} = \frac{1}{2.1}[0.4 + (\frac{200\mu_g V_{g,in}}{d_p^2(\rho_s - \rho_g)g})^{1/3}] \tag{55}$$

5. Calculate the particle terminal velocity from the following equation [2]:

$$u_t = \left[-3.809 + \left(3.809^2 + 1.832 Ar^{0.5} \right)^{0.5} \right]^2 \frac{\mu_g}{\rho_g d_p} \tag{56}$$

6. Specify stability of fluidized bed.

7. Determine the Δt, Δx and Δy

8. Determine the fluidized bed height at the entering velocity using the equation [5]:

$$H1 = \frac{\left(1 - \varepsilon_{g,mf}\right)}{\left(1 - \varepsilon_{g,in}\right)} H_{mf} \tag{57}$$

9. Specify Initial and boundary conditions.

10. Call subroutine "cont" to solve particles phase continuity equations and evaluate the new time step particles volume fractions (ε_s^{n+1}) consequently evaluate (ε_g^{n+1}) from equation (41).

Note: we use the excess solid volume correction [8] in a special subroutine:

The correction works out as a posteriori redistribution of the particle phase volume fraction in excess in each cell where:

$$\varepsilon_s \le \varepsilon_{s,\max} \tag{58}$$

$$\varepsilon_{s,\max} = 1 - \varepsilon_{g,mf} \tag{59}$$

and if $\varepsilon_s > \varepsilon_{s,\max}$then:

$$\varepsilon_s^{ex} = \varepsilon_s - \varepsilon_{s,\max} \tag{60}$$

The balance may be expressed in terms of particle volume fraction:

$$\varepsilon_{s,i,j}^{new} = \varepsilon_{s,i,j}^{old} - \varepsilon_{s,i,j}^{ex} + \frac{\varepsilon_{s,i+1,j}^{ex}}{4} + \frac{\varepsilon_{s,i-1,j}^{ex}}{4} + \frac{\varepsilon_{s,i,j+1}^{ex}}{4} + \frac{\varepsilon_{s,i,j-1}^{ex}}{4} \tag{61}$$

Figure (3) shows the correction mechanism:

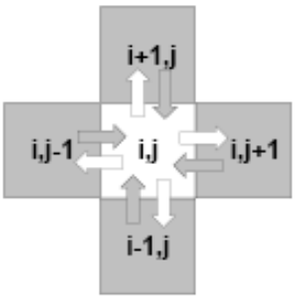


Figure 3. The excess solid volume correction

11. Call subroutine "dirx" to solve momentum equation in x-direction and evaluate at the new time step x-components velocities ($u_g^{n+1} and\ u_s^{n+1}$). In this subroutine, equations (14) and (43) are solved to get values of x-component new step velocities ($u_g^{n+1} and\ u_s^{n+1}$). Equation (43) is reduced to the following form :

$$A_{11}(u_s)_{i,j}^{n+1} + A_{12}(u_g)_{i,j}^{n+1} = A_{13} \tag{62}$$

where:

$$A_{11} = \frac{\rho_s}{\Delta t} \tag{63}$$

$$A_{12} = \frac{\rho_g}{\Delta t} \tag{64}$$

$$
\begin{aligned}
A_{13} &= \frac{\rho_s}{\Delta t}\left(u_s\right)_{i,j}^{n} + \frac{\rho_g}{\Delta t}\left(u_g\right)_{i,j}^{n} \\
&-\frac{\left(u_s\right)_{i,j}^{n}}{\Delta x}\begin{cases}\left(u_s\right)_{i,j}^{n} - \left(u_s\right)_{i-1,j}^{n} & ,if\left(u_s\right)_{i,j}^{n} \geq 0.0 \\ \left(u_s\right)_{i+1,j}^{n} - \left(u_s\right)_{i,j}^{n} & ,if\left(u_s\right)_{i,j}^{n} < 0.0\end{cases} \\
&-\frac{\left(v_s\right)_{i,j}^{n}}{\Delta y}\begin{cases}\left(u_s\right)_{i,j}^{n} - \left(u_s\right)_{i,j-1}^{n} & ,if\left(v_s\right)_{i,j}^{n} \geq 0.0 \\ \left(u_s\right)_{i,j+1}^{n} - \left(u_s\right)_{i,j}^{n} & ,if\left(v_s\right)_{i,j}^{n} < 0.0\end{cases} \\
&-\frac{\left(u_g\right)_{i,j}^{n}}{\Delta x}\begin{cases}\left(u_g\right)_{i,j}^{n} - \left(u_g\right)_{i-1,j}^{n} & ,if\left(u_g\right)_{i,j}^{n} \geq 0.0 \\ \left(u_g\right)_{i+1,j}^{n} - \left(u_g\right)_{i,j}^{n} & ,if\left(u_g\right)_{i,j}^{n} < 0.0\end{cases} \\
&-\frac{\left(v_g\right)_{i,j}^{n}}{\Delta y}\begin{cases}\left(u_g\right)_{i,j}^{n} - \left(u_g\right)_{i,j-1}^{n} & ,if\left(v_g\right)_{i,j}^{n} \geq 0.0 \\ \left(u_g\right)_{i,j+1}^{n} - \left(u_g\right)_{i,j}^{n} & ,if\left(v_g\right)_{i,j}^{n} < 0.0\end{cases}
\end{aligned}
\tag{65}
$$

so equation (62) and equation (14) result the following system of equations:

$$
\begin{pmatrix} A_{11} & A_{12} \\ \left(\varepsilon_s\right)_{i,j}^{n+1} & \left(\varepsilon_g\right)_{i,j}^{n+1} \end{pmatrix}\begin{pmatrix} \left(u_s\right)_{i,j}^{n+1} \\ \left(u_g\right)_{i,j}^{n+1} \end{pmatrix} = \begin{pmatrix} A_{13} \\ U_{gin} \end{pmatrix}
$$

Which are solved to get ($u_g^{n+1} and\ u_s^{n+1}$)

12. Call subroutine "diry" to solve momentum equation in y-direction and evaluate at the new time step y-components velocities ($v_g^{n+1} and\ v_s^{n+1}$). In this subroutine, equations (13) and (44) are used to get values of ($v_g^{n+1} and\ v_s^{n+1}$). Equation (44) is reduced to the following form :

$$
B_{11}(v_s)_{i,j}^{n+1} + B_{12}(v_g)_{i,j}^{n+1} = B_{13} \tag{66}
$$

where:

$$
B_{11} = \frac{\rho_s}{\Delta t} + \beta\left(1 + \frac{\left(\varepsilon_s\right)_{i,j}^{n}}{\left(1 - \left(\varepsilon_s\right)_{i,j}^{n}\right)}\right) \tag{67}
$$

where:

$$\beta = C_d \frac{3\left(\varepsilon_s\right)_{i,j}^n \rho_g \left|\left(v_g\right)_{i,j}^n - \left(v_s\right)_{i,j}^n\right|}{4d_p}\left(1-\left(\varepsilon_s\right)_{i,j}^n\right)^{-1.8} \tag{68}$$

$$B_{12} = -\frac{\rho_g}{\Delta t} - \beta\left(1+\frac{\left(\varepsilon_s\right)_{i,j}^n}{\left(1-\left(\varepsilon_s\right)_{i,j}^n\right)}\right) \tag{69}$$

$$\begin{aligned}
B_{13} &= \frac{\rho_s}{\Delta t}\left(v_s\right)_{i,j}^n + \frac{\rho_g}{\Delta t}\left(v_g\right)_{i,j}^n \\
&-\frac{\left(u_s\right)_{i,j}^n}{\Delta x}\begin{cases}\left(v_s\right)_{i,j}^n - \left(v_s\right)_{i-1,j}^n & ,if\left(u_s\right)_{i,j}^n \geq 0.0\\ \left(v_s\right)_{i+1,j}^n - \left(v_s\right)_{i,j}^n & ,if\left(u_s\right)_{i,j}^n < 0.0\end{cases} \\
&-\frac{\left(v_s\right)_{i,j}^n}{\Delta y}\begin{cases}\left(v_s\right)_{i,j}^n - \left(v_s\right)_{i,j-1}^n & ,if\left(v_s\right)_{i,j}^n \geq 0.0\\ \left(v_s\right)_{i,j+1}^n - \left(v_s\right)_{i,j}^n & ,if\left(v_s\right)_{i,j}^n < 0.0\end{cases} \\
&-\frac{\left(u_g\right)_{i,j}^n}{\Delta x}\begin{cases}\left(v_g\right)_{i,j}^n - \left(v_g\right)_{i-1,j}^n & ,if\left(u_g\right)_{i,j}^n \geq 0.0\\ \left(v_g\right)_{i+1,j}^n - \left(v_g\right)_{i,j}^n & ,if\left(u_g\right)_{i,j}^n < 0.0\end{cases} \\
&-\frac{\left(v_g\right)_{i,j}^n}{\Delta y}\begin{cases}\left(v_g\right)_{i,j}^n - \left(v_g\right)_{i,j-1}^n & ,if\left(v_g\right)_{i,j}^n \geq 0.0\\ \left(v_g\right)_{i,j+1}^n - \left(v_g\right)_{i,j}^n & ,if\left(v_g\right)_{i,j}^n < 0.0\end{cases} \\
&-\frac{\left(\varepsilon_s\right)_{i,j}^n - \left(\varepsilon_s\right)_{i,j-1}^n}{dy}\left(3.2gd_p\left(\rho_s - \rho_g\right)\right)
\end{aligned} \tag{70}$$

So equation (66) and equation (13) result the following system of equations:

$$\begin{pmatrix} B_{11} & B_{12} \\ \left(\varepsilon_s\right)_{i,j}^{n+1} & \left(\varepsilon_g\right)_{i,j}^{n+1}\end{pmatrix}\begin{pmatrix}\left(v_s\right)_{i,j}^{n+1} \\ \left(v_g\right)_{i,j}^{n+1}\end{pmatrix} = \begin{pmatrix} B_{13} \\ V_{gin}\end{pmatrix}$$

Which are solved to get $\left(v_g^{n+1} and\ v_s^{n+1}\right)$

13. Call subroutine "temp" to solve energy equation and evaluate the new time step gas and solid particles temperatures $\left(T_g^{n+1} and\ T_s^{n+1}\right)$.In this subroutine, equations (46) and (47) are

used to get values of new time step temperatures for both phases (T_g^{n+1} *and* T_s^{n+1}). Equation (46) is reduced to the following form :

$$C_{11}(T_s)_{i,j}^{n+1} + C_{12}(T_g)_{i,j}^{n+1} = C_{13} \tag{71}$$

where:

$$C_{11} = \frac{\rho_s C_{p,s}}{\Delta t}\left(\varepsilon_s^{n+1}\right) + \left(h_v\right)_{i,j}^{n+1} \tag{72}$$

$$C_{12} = \left(h_v\right)_{i,j}^{n+1} \tag{73}$$

$$\begin{aligned} C_{13} &= \frac{\rho_s C_{p,s}}{\Delta t}\left(\varepsilon_s T_s\right)_{i,j}^{n} \\ &- \frac{\rho_s C_{p,s}\left(u_s\right)_{i,j}^{n}}{\Delta x}\begin{cases}\left(\varepsilon_s T_s\right)_{i,j}^{n} - \left(\varepsilon_s T_s\right)_{i-1,j}^{n} & ,if\left(u_s\right)_{i,j}^{n} \geq 0.0 \\ \left(\varepsilon_s T_s\right)_{i+1,j}^{n} - \left(\varepsilon_s T_s\right)_{i,j}^{n} & ,if\left(u_s\right)_{i,j}^{n} < 0.0\end{cases} \\ &- \frac{\rho_s C_{p,s}\left(v_s\right)_{i,j}^{n}}{\Delta y}\begin{cases}\left(\varepsilon_s T_s\right)_{i,j}^{n} - \left(\varepsilon_s T_s\right)_{i,j-1}^{n} & ,if\left(v_s\right)_{i,j}^{n} \geq 0.0 \\ \left(\varepsilon_s T_s\right)_{i,j+1}^{n} - \left(\varepsilon_s T_s\right)_{i,j}^{n} & ,if\left(v_s\right)_{i,j}^{n} < 0.0\end{cases} \\ &+ \frac{\left(\varepsilon_s K_s T_s\right)_{i+1,j}^{n} - 2\left(\varepsilon_s K_s T_s\right)_{i,j}^{n} + \left(\varepsilon_s K_s T_s\right)_{i-1,j}^{n}}{\Delta x^2} \\ &+ \frac{\left(\varepsilon_s K_s T_s\right)_{i,j+1}^{n} - 2\left(\varepsilon_s K_s T_s\right)_{i,j}^{n} + \left(\varepsilon_s K_s T_s\right)_{i,j-1}^{n}}{\Delta y^2} + \left(\varepsilon_s \dot{q}\right)_{i,j}^{n} \end{aligned} \tag{74}$$

Also equation (47) is reduced to the following form:

$$D_{11}(T_s)_{i,j}^{n+1} + D_{12}(T_g)_{i,j}^{n+1} = D_{13} \tag{75}$$

where:

$$D_{11} = \left(h_v\right)_{i,j}^{n+1} \tag{76}$$

http://dx.doi.org/10.5772/52072

$$D_{12} = \frac{\rho_g C_{p,g}}{\Delta t}\left(\varepsilon_g^{n+1}\right) + \left(h_v\right)_{i,j}^{n+1} \tag{77}$$

$$\begin{aligned} D_{13} &= \rho_g C_{p,g} \frac{\left(\varepsilon_g T_g\right)_{i,j}^{n}}{\Delta t} \\ &- \frac{\rho_g C_{p,g}\left(u_g\right)_{i,j}^{n}}{\Delta x}\begin{cases} \left(\varepsilon_g T_g\right)_{i,j}^{n} - \left(\varepsilon_g T_g\right)_{i-1,j}^{n} & ,if\left(u_g\right)_{i,j}^{n} \geq 0. \\ \left(\varepsilon_g T_g\right)_{i+1,j}^{n} - \left(\varepsilon_g T_g\right)_{i,j}^{n} & ,if\left(u_g\right)_{i,j}^{n} < 0.0 \end{cases} \\ &- \frac{\rho_s C_{p,g}\left(v_g\right)_{i,j}^{n}}{\Delta y}\begin{cases} \left(\varepsilon_g T_g\right)_{i,j}^{n} - \left(\varepsilon_g T_g\right)_{i,j-1}^{n} & ,if\left(v_g\right)_{i,j}^{n} \geq 0.0 \\ \left(\varepsilon_g T_g\right)_{i,j+1}^{n} - \left(\varepsilon_g T_g\right)_{i,j}^{n} & ,if\left(v_g\right)_{i,j}^{n} < 0.0 \end{cases} \\ &+ \frac{\left(\varepsilon_g K_g T_g\right)_{i+1,j}^{n} - 2\left(\varepsilon_g K_g T_g\right)_{i,j}^{n} + \left(\varepsilon_g K_g T_g\right)_{i-1,j}^{n}}{\Delta x^2} \\ &+ \frac{\left(\varepsilon_g K_g T_g\right)_{i,j+1}^{n} - 2\left(\varepsilon_g K_g T_g\right)_{i,j}^{n} + \left(\varepsilon_g K_g T_g\right)_{i,j-1}^{n}}{\Delta y^2} \end{aligned} \tag{78}$$

so equation (71) and equation (75) result the following system of equations:

$$\begin{pmatrix} C_{11} & C_{12} \\ D_{11} & D_{12} \end{pmatrix}\begin{pmatrix} (T_s)_{i,j}^{n+1} \\ (T_g)_{i,j}^{n+1} \end{pmatrix} = \begin{pmatrix} C_{13} \\ D_{13} \end{pmatrix}$$

Which are solved to get ($T_g^{n+1} and\ T_s^{n+1}$)

14. Make gas residual check,which given from the equation (42):

- If $|d_g(i,\ j)| \leq \delta$ go to step 15, where δ is a small positive value δ=5X10$^{-3.}$
- Else adjust $\varepsilon_g^{n+1}$by :

$$\begin{aligned} \left(\varepsilon_g\right)_{i,j}^{n+1} &= \left(\varepsilon_g\right)_{i,j}^{n} - \frac{dt}{\Delta x}\left(u_g\right)_{i,j}^{n+1}\begin{cases} \left(\varepsilon_g\right)_{i,j}^{n+1} - \left(\varepsilon_g\right)_{i-1,j}^{n+1} & ,if\left(u_g\right)_{i,j}^{n+1} \geq 0.0 \\ \left(\varepsilon_g\right)_{i+1,j}^{n+1} - \left(\varepsilon_g\right)_{i,j}^{n+1} & ,if\left(u_g\right)_{i,j}^{n+1} < 0.0 \end{cases} \\ &- \frac{\Delta t}{\Delta y}\left(v_g\right)_{i,j}^{n+1}\begin{cases} \left(\varepsilon_g\right)_{i,j}^{n+1} - \left(\varepsilon_g\right)_{i,j-1}^{n+1} & ,if\left(v_g\right)_{i,j}^{n+1} \geq 0.0 \\ \left(\varepsilon_g\right)_{i,j+1}^{n+1} - \left(\varepsilon_g\right)_{i,j}^{n+1} & ,if\left(v_g\right)_{i,j}^{n+1} < 0.0 \end{cases} \end{aligned} \tag{79}$$

and calculate ε_s^{n+1} from equation (41).

- Go to step 11 and calculate new time step velocities

15. Calculate the gas pressure values.

16. Calculate dimensionless numbers.

17. End program.

8. Parametric study of the hydrodynamic and thermal results

The present work results show the effect of variation of several bed parameters such as particle diameter, terminal velocity of the particle, minimum fluidized velocity of the particle input gas velocity, fluidized material type and heat generation by particles on the hydrodynamic and thermal behavior of fluidized bed. In this section the effect of different parameters in hydrodynamic and thermal performance of fluidized bed is analyzed in detail.

8.1. Effect of particle diameter

Particle diameter is the most influential parameter in the overall fluidized bed performance. In view of that fact, the bed material in a fluidized bed is characterized by a wide range of particle diameter, so that the effect of particle diameter is analyzed in details. In this section particle diameter is changed from 100 μm to 1000 μm for sand as fluidized material to study the effect of particle diameter on the fluidization performance.

One of the important parameter of the fluidized bed study is the total pressure drop across the bed. Although it is constant after beginning of fluidization and equal to the weight of the bed approximately. But its value changes with change of particle diameter.The effect of change of particle diameter on total pressure drop is very important in design and cost of fluidized bed. Figure (4) shows that effect for sand particles of different diameters (100, 200, 300, 400, 500, 600, 700, 800, 900 and 1000 μm). It is clear that the pressure drop increase with increase of particle diameter, which means that small particle is betters in design of fluidized bed cost.

A key parameter in the Thermal analysis of fluidized bed is the average heat transfer coefficient. Figure (5) shows the variation of average heat transfer coefficient with the time for different particles diameter from 100 to 1000 μm sand particles.It is observed from the figure that particles with small size show higher values of average heat transfer coefficient. The particles with diameter 100 μm show higher for average heat transfer coefficient reaches to about 3 times of particles with diameter 1000 μm.

Particles diameter determines the type of particles on Geldart diagram, consequently the behavior of the fluidized bed.

Figures from (6) to (13) illustrate the effect of particles diameter on hydrodynamic and thermal behavior for particle type-B. These figures explain the high disturbance in different bed

http://dx.doi.org/10.5772/52072

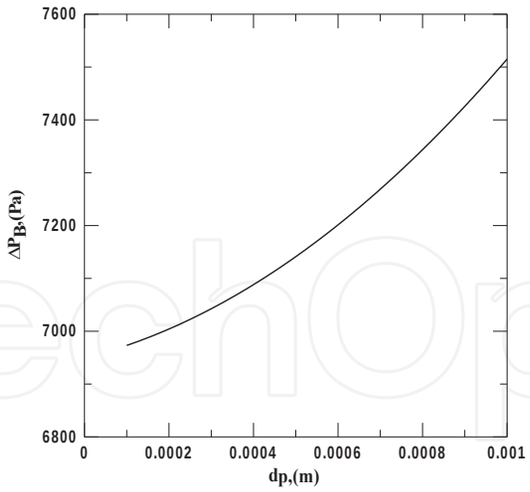


Figure 4. Effect of particle diameter on total pressure drop across fluidized bed

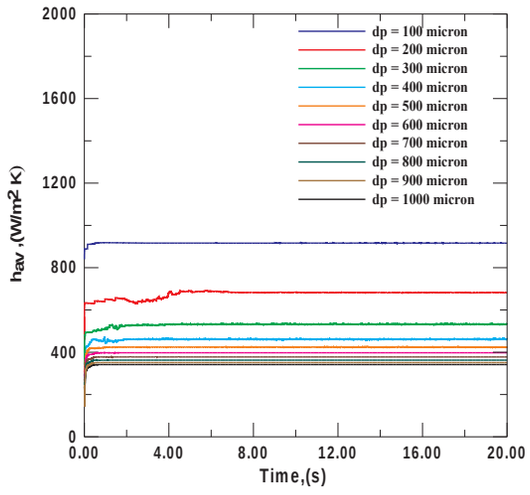
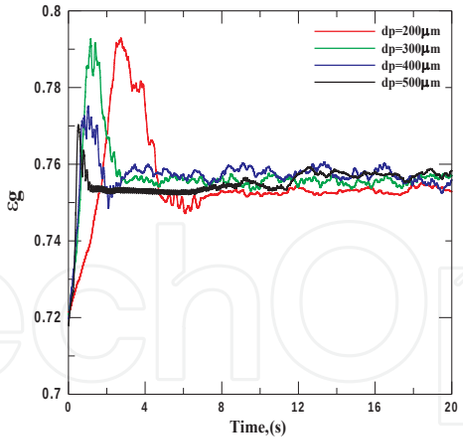


Figure 5. Effect of particle diameter on average heat transfer coefficient in fluidized bed

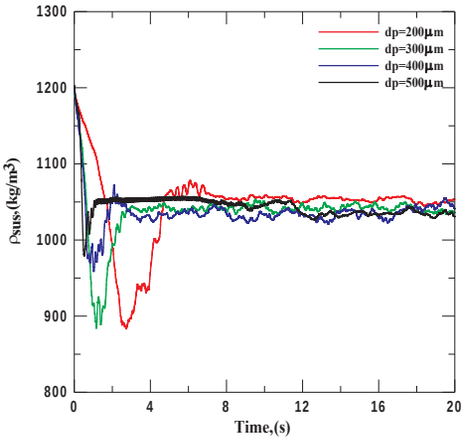
parameters (ε_g, ϱ_{sus},v_g,v_s,u_g,u_s,T_g,T_s) due to the bubbles formation. The disturbance decreases with increase of particles diameter. This may be due to come near D-type under uniform fluidization.

Fluidized bed is used for wide range of particle diameter. It is better to fluidize particle Dtype in spouted bed to decrease the pressure drop. However, using uniform fluidization for D type give a good and stable thermal behavior of fluidized bed. So in some applications like nuclear reactors the stability and safety is important than cost of pumping power.

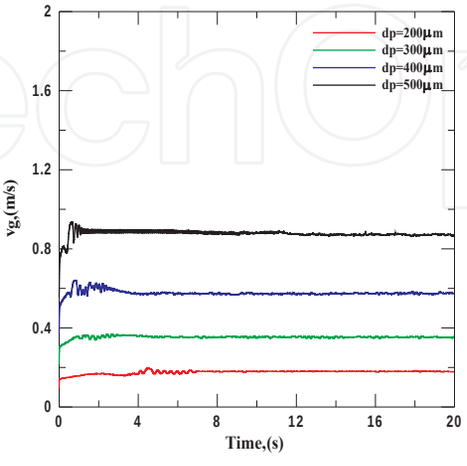
Figures from (14) to (21) show the effect of change particle diameter on hydrodynamic and thermal behavior for particle D-type. For this particles type, the behavior of fluidized bed is more uniform in performance than B-type [be consistent with usage and define what the different types are]. Although D-type gives butter fluidization in spouted bed but it gives good performance under uniform fluidization with high pressure drop as shown in figure (4). This means an increase in pumping power and costs to achieve uniform fluidization.



)LJXUH(II HFW RI SDUWLFOH GLDPHWHU RQ JDV YROXPH IUDFWLRQ % W\SH



)LJXUH(II HFW RI SDUWLFOH GLDPHWHU RQ VXVSHQVLRQ GHQVLW\ % W\SH



)LJXUH(II HFW RI SDUWLFOH GLDPHWHU RQ YHUWLFDO JDV YHORFLW\ % W\SH